

Article

Limiting Performance of the Ejector Refrigeration Cycle with Pure Working Fluids

Jiawei Fu, Zhenhua Liu, Xingyang Yang *, Sumin Jin and Jilei Ye

School of Energy Science and Engineering, Nanjing Tech University, Nanjing 211816, China

* Correspondence: yangxy@njtech.edu.cn; Tel.: +86-25-58139661

Abstract: An ejector refrigeration system is a promising heat-driven refrigeration technology for energy consumption. The ideal cycle of an ejector refrigeration cycle (ERC) is a compound cycle with an inverse Carnot cycle driven by a Carnot cycle. The coefficient of performance (COP) of this ideal cycle represents the theoretical upper bound of ERC, and it does not contain any information about the properties of working fluids, which is a key cause of the large energy efficiency gap between the actual cycle and the ideal cycle. In this paper, the limiting COP and thermodynamics perfection of subcritical ERC is derived to evaluate the ERC efficiency limit under the constraint of pure working fluids. 15 pure fluids are employed to demonstrate the effects of working fluids on limiting COP and limiting thermodynamics perfection. The limiting COP is expressed as the function of the working fluid thermophysical parameters and the operating temperatures. The thermophysical parameters are the specific entropy increase in the generating process and the slope of the saturated liquid, and the limiting COP increases with these two parameters. The result shows R152a, R141b, and R123 have the best performance, and the limiting thermodynamic perfections at the referenced state are 86.8%, 84.90%, and 83.67%, respectively.

Keywords: ejector refrigeration cycle; working fluids; fluid thermophysical property; thermodynamics



Citation: Fu, J.; Liu, Z.; Yang, X.; Jin, S.; Ye, J. Limiting Performance of the Ejector Refrigeration Cycle with Pure Working Fluids. *Entropy* **2023**, *25*, 223. <https://doi.org/10.3390/e25020223>

Academic Editor: Lei Wang

Received: 28 December 2022

Revised: 17 January 2023

Accepted: 21 January 2023

Published: 24 January 2023



Copyright: © 2023 by the authors. Licensee MDPI, Basel, Switzerland. This article is an open access article distributed under the terms and conditions of the Creative Commons Attribution (CC BY) license (<https://creativecommons.org/licenses/by/4.0/>).

1. Introduction

Refrigeration has become a very important part of modern society, and refrigeration consumes more than 20% of the overall electricity used worldwide [1]. Therefore, many scholars have tried to develop non-electric-driven refrigeration systems. Among these cooling technologies, ejector refrigeration cycles (ERCs) are regarded as promising, for their simple structure, lack of moving parts, low capital and maintenance costs, and long lifespan [2]. They can be driven by a low-temperature heat source, but their low-performance coefficient makes it hard to penetrate the commercial market. Compared with the ideal cycle (as shown in Figure 1), the thermodynamics perfection of an actual ERC is less than 50%, according to the statistical results of experimental data [3].

An ERC is driven by a heat source. It consists of an ejector, a condenser, a pump, a generator, an expansion valve, and an evaporator, as shown in Figure 1. The ejector is a device that uses high-pressure flow to entrain low-pressure flow for mixing pressure. The working fluid at the outlet of the ejector is condensed in the condenser and divided into two parts. The primary flow is pumped in the pump, evaporates in the generator, and then expands in the ejector nozzle. The secondary flow expands in the expansion valve, and evaporates in the evaporator. Then, the vapor from the evaporator is compressed in the ejector by the primary flow.

For the ideal cycle, all the processes are reversible. Its coefficient of performance (COP) is only related to the temperatures of the heat source, heat sink, and cold media. While for an actual ERC, there are different kinds of irreversible losses in it, most of which are related to working fluids. Moreover, its COP is not only related to the working conditions, but also to the working fluid properties. Since French engineer Maurice Leblanc introduced the

steam ejector refrigeration system in 1910 [4], ERCs have been continuously developing for more than a century. In the past hundred years, a huge number of refrigerants have been applied in ERCs. In the early 1900s, the working fluid was mainly water. Since the 1930s, halocarbon refrigerants have been extensively researched in ERCs both theoretically and experimentally. For example, R11 [5], R12 [6], R113 [7], R123 [5], R134a [8], R141b [9], R142b [10], R152a [11], and R245fa [12]. As the Montreal Protocol on substances that deplete the ozone layer was ratified in 1987, scholars turned their research to natural refrigerants and hydrocarbon refrigerants, such as water [13], ammonia [14], R290 [15], R600 [16], R600a [17], etc.

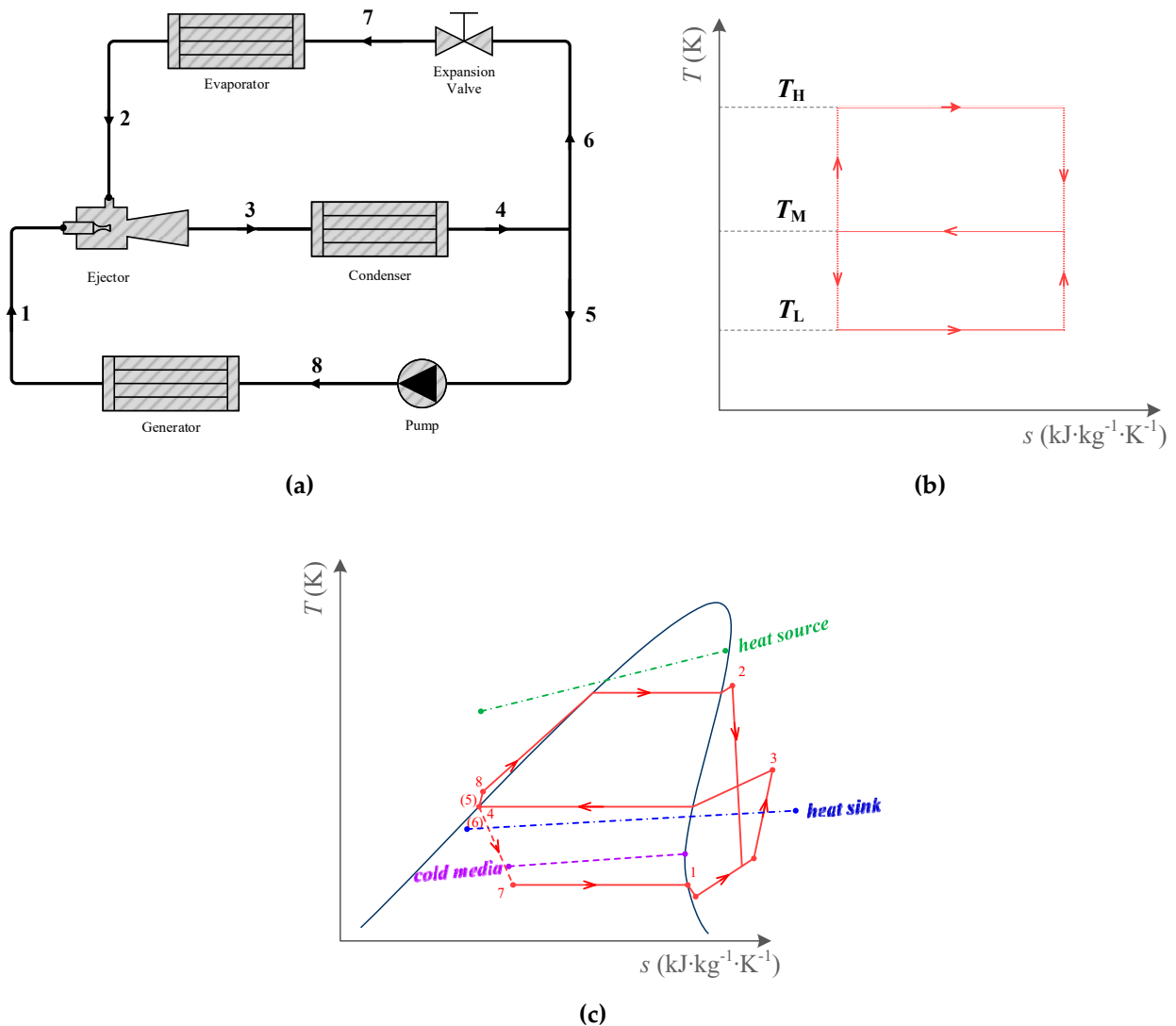


Figure 1. The ejector refrigeration cycle (ERC): (a). The schematic for ERC; (b). The T-s diagram of ERC ideal cycle; (c). The T-s diagram of practical ERC.

To screen the suitable fluids, many scholars have explored the relationship between working fluid thermophysical property parameters and cycle or process performance. Zheng et al. [18] found the parameter ζ of the relative heat loss ratio between a zeotropic mixture and heat transfer fluid. This parameter can reflect the irreversible loss during constant pressure evaporation or condensation, and the parameter can be used as a criterion for the selection of zeotropic working fluids in the heat transfer process. Yang et al. [19] linked the heat transfer process with the thermodynamic behavior of heat exchangers and defined the non-dimensional integration temperature difference of pure working fluid in the heat exchanger. It is useful for the performance evaluation of the heat exchanger.

For the compression process of the pump, Xu et al. [20] proposed a parameter $\alpha_v/(\rho c_p)$ to identify the influence of the physical properties of working fluid on the performance of the pump. The result showed that the isentropic efficiency of the pump decreases with the increment of $\alpha_v/(\rho c_p)$ of different working fluids. For the process of the ejector, Chen et al. [21] found that the slope of the saturated vapor line in the T - s diagram of the working fluid has a significant effect on ejector performance. The ejector has better performance when using dry working fluid. Similar results are found in the research from Mwesigye and Dworkin [16]. Buyadgie et al. [22] proposed a criterion of working fluids selection for ERC based on criteria of the significant difference in molecular weights of working fluids. For cycle performance, a fluid with a high molecular weight is a good choice. Kasperski and Gil [23,24] studied the relationship between the normal boiling temperature of refrigerants and system performance. It is found that the refrigerants with lower normal boiling temperatures have better efficiency in the system. Śmierciew et al. [25] proposed a compression efficiency η_c related to the specific heat of the vaporization of the working fluid and the working pressure used to assess the performance of the ejection refrigeration cycle. It is concluded that the above literature mainly explores the relationship between the practical COP of ERC and working fluid properties, under the constraints of different working conditions. To the authors' best knowledge, scant research has been conducted to investigate the COP limit of ERC by considering the working fluid properties.

In this paper, to evaluate the cycle performance upper limit under the constraint of pure working fluids, a limiting ejector refrigeration cycle (LERC) is developed. It is the closest cycle to the ideal cycle that can be achieved by the practical cycle, only taking the influence of working fluid thermophysical properties into account. The COP of LERC (COP_{limit}) represents the maximum COP that can be achieved by the actual ERC when only considering the effect of working fluids, and the calculation method of COP_{Limit} is proposed. Moreover, the limiting performance of ERC with different working fluids is analyzed. This paper is organized as follows: in Section 2, the definition of LERC and the COP_{limit} methodology are presented. In Section 3, the effects of working fluids and working conditions on the LERC performance are analyzed. In Section 4, the main conclusions are presented.

2. Methodology

2.1. Fluid Classification and Fluid Slope

In the existing literature, according to the slope of the dry saturated vapor line in the T - s diagram, the working fluids are divided into three categories: dry working fluids ($dT/ds > 0$), isentropic working fluids ($dT/ds = \infty$), and wet working fluids ($dT/ds < 0$). Dry or isentropic working fluids are more suitable for the ejector because when wet working fluids expand in the ejector, liquid droplets may be formed, resulting in the performance degradation of the ejector. However, superheat can solve this problem. Strictly speaking, there is almost no isentropic working fluid in pure fluids, but some working fluids are approximately regarded as isentropic working fluids, such as R142b, R1234yf, etc.

In this research, the slope of the working fluid in a saturated state is obtained by the following method. According to the basic thermodynamic equations, there is

$$ds = \frac{c_p}{T} dT - \left(\frac{\partial v}{\partial T} \right)_p dp \quad (1)$$

When the fluid is in a vapor–liquid two-phase equilibrium state, according to the Clapeyron equation, there is

$$\frac{dp}{dT} = \frac{h_{L-V}}{T_s(v_V - v_L)} \quad (2)$$

where h_{L-V} is specific heat of evaporation, v is the specific volume, and the subscripts V and L refer to saturated vapor and saturated liquid, respectively. Combining Equations (2) and (1), there is

$$ds = \frac{c_p}{T} dT_s - \frac{\alpha h_{L-V} v}{T_s (v_V - v_L)} dT \tag{3}$$

where α is the thermal expansion coefficient

$$\alpha = \frac{1}{v} \left(\frac{\partial v}{\partial T} \right)_p \tag{4}$$

Therefore, the slope of the saturated liquid or vapor line in the T - s diagram of the working fluid can be expressed as:

$$\beta = \frac{dT}{ds} = \frac{T_s}{c_p - \frac{\alpha h_{L-V} v}{v_V - v_L}} \tag{5}$$

The saturated vapor slope β of 15 pure fluids is shown in Figure 2. For wet fluids, the slope decreases first and then increases as the reduced temperature T_r ($T_r = T_s / T_{cr}$) increases from 0.555 to 0.995. They all get a minimal value as T_r is about 0.82. For isentropic fluids and dry fluids, there are two pole points. The slope decreases first and then increases as T_r increases between these two points, but it decreases as T_r increases when it is outside this range.

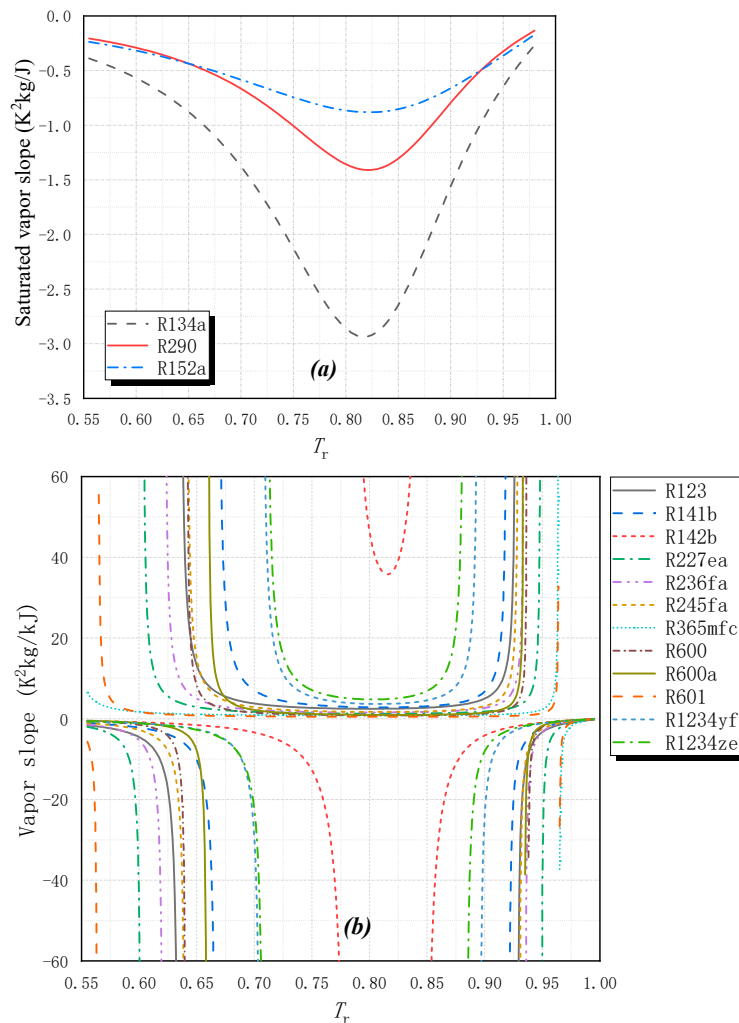


Figure 2. The slope of the saturated vapor in T - s diagram for pure fluids: (a) wet fluids, (b) isentropic fluids and dry fluids.

2.2. Limiting ERC

To quantify the influence of the fluid thermophysical properties on the cycle performance, the following assumptions are made in this paper:

- (1) The heat exchange processes are idealized. The temperature of the heat source and heat sink is constant. In the generator, the highest temperature of the working fluid is equal to the heat source temperature. The condensing temperature is equal to the heat sink temperature, and the evaporating temperature is equal to the cold media temperature.
- (2) Irreversibility in other processes of the cycle is ignored, such as the compression process in the pump, and the expansion, mixing, and diffusion process in the ejector are all regarded as isentropic processes, etc.

Under the above assumptions, it can be concluded that the gap between the ideal ERC and actual ERC is caused by the property of the working fluid, as shown in Figure 3, represented by the gray area. It can be seen that the gap is mainly composed of three parts: (1) the heat transfer process in the generator when the fluid is heated from a subcooled state to a saturated liquid state; (2) the heat transfer process in the generator as the fluid is heated from a saturated vapor state to a superheated state; (3) the heat transfer process in the condenser when the fluid is cooled from a superheated gas state to a saturated liquid state. For dry fluid, the loss is caused by (1) and (3). For isentropic fluid, the gap is caused by (1), and for wet fluid, it is caused by (1), (2), and (3).

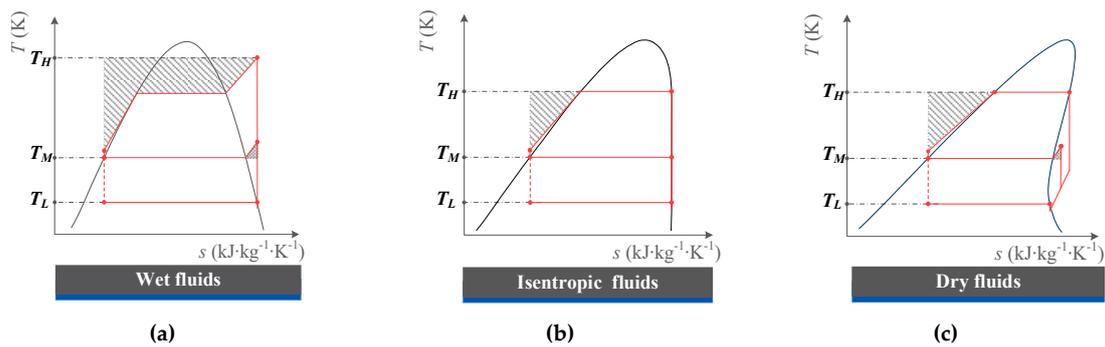


Figure 3. T-s Diagram of ERC with different fluids: (a) Wet fluids; (b) Isentropic fluids; (c) Dry fluids.

To evaluate the upper limit of the cycle with actual pure fluid, a cycle that is defined as a limiting ejector refrigeration cycle (LERC) is proposed in this paper. For dry fluids, the irreversible loss in the non-isothermal condensation process is ignored, when it is cooled from superheated gas to saturated vapor. For wet fluids, part of the irreversible loss in the non-isothermal generating process is neglected, when it is heated from saturated vapor to superheated gas. The diagram of LERC for different fluids is shown in Figure 4. Based on the thermodynamic graphical analysis method, the limiting COP is obtained.

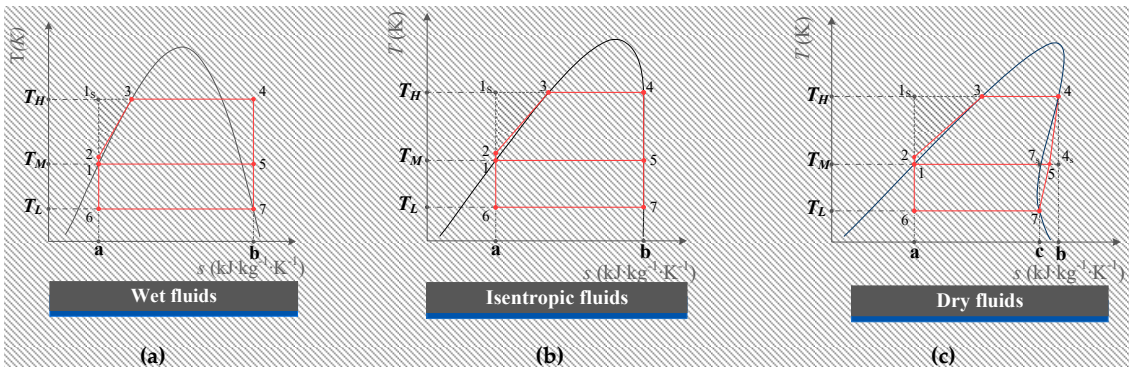


Figure 4. T-s Diagram of LERC with different fluids: (a) Wet fluids; (b) Isentropic fluids; (c) Dry fluids.

2.3. Limiting COP

For ERC, the COP can be expressed as:

$$COP = \frac{\dot{Q}_{ev}}{\dot{Q}_{ge}} = \frac{\dot{m}_{ev}q_{ev}}{\dot{m}_{ge}q_{ge}} = \mu \frac{q_{ev}}{q_{ge}} \tag{6}$$

where the subscripts ev and ge represent the evaporation process and the generation process, respectively, and μ is the entrainment ratio, the flow rate ratio between the secondary fluid and the primary:

$$\mu = \frac{\dot{m}_s}{\dot{m}_p} = \frac{\dot{m}_{ev}}{\dot{m}_{ge}} \tag{7}$$

Neglecting the pump power consumption, there is

$$\dot{Q}_{ev} + \dot{Q}_{ge} = \dot{Q}_{co} \tag{8}$$

$$\dot{m}_{ev}q_{ev} + \dot{m}_{ge}q_{ge} = \dot{m}_{co}q_{co} \tag{9}$$

According to the mass conservation equation, there is

$$\dot{m}_{ev} + \dot{m}_{ge} = \dot{m}_{co} \tag{10}$$

Combining Equations (7), (9), and (10), there is

$$\mu = \frac{q_{ge} - q_{co}}{q_{co} - q_{ev}} \tag{11}$$

When Equation (11) is brought into Equation (6), there is

$$COP = \frac{q_{ge} - q_{co}}{q_{co} - q_{ev}} \cdot \frac{q_{ev}}{q_{ge}} = \frac{q_{ev}}{q_{co} - q_{ev}} \cdot \frac{q_{ge} - q_{co}}{q_{ge}} = \left(\frac{q_{ev}}{q_{co} - q_{ev}} \right) \left(1 - \frac{q_{co}}{q_{ge}} \right) \tag{12}$$

2.3.1. Wet Fluids and Isentropic Fluids

According to the thermodynamic geometric analysis method, the limiting COP can be expressed as an expression of the geometric area as shown in Figure 4. Then, the limiting COP can be expressed as

$$COP'_{limit} = \left(1 - \frac{q'_{co}}{q'_{ge}} \right) \left(\frac{q'_{ev}}{q'_{co} - q'_{ev}} \right) = \left(1 - \frac{A_{1-5-b-a-1}}{A_{1-3-4-b-a-1}} \right) \cdot \frac{A_{6-7-b-a-6}}{A_{1-5-7-6-1}} \tag{13}$$

where

$$q'_{ev} = A_{6-7-b-a-6} = T_L(s_b - s_a) = T_L \cdot \Delta s_{a-b} \tag{14}$$

$$q'_{co} = A_{1-5-b-a-1} = T_M(s_b - s_a) = T_M \cdot \Delta s_{a-b} \tag{15}$$

$$q'_{ge} = A_{1-3-4-b-a-1} = A_{1s-4-b-a-1s} - A_{1s-3-1-1s} \tag{16}$$

and $A_{1s-4-b-a-1s}$ is the input heat for constant temperature heat source:

$$A_{1s-4-b-a-1s} = T_H \cdot \Delta s_{a-b} \tag{17}$$

$$A_{1s-3-1-1s} \approx \frac{1}{2\beta} (T_H - T_M)^2 \tag{18}$$

where β is the slope of the tangent line at state 1 and it can be calculated by formula (5). Although the tangent line does not completely coincide with the saturated liquid line,

the difference is very small and neglected. Δs_{a-b} is the specific entropy increase in the generating process. Substituting Equations (17)–(21) into (16), there is:

$$COP'_{\text{limit}} = \frac{T_L}{T_M - T_L} \bullet \left(1 - \frac{T_M}{T_H - \frac{(T_H - T_M)^2}{2\beta \cdot \Delta s_{a-b}}} \right) \tag{19}$$

2.3.2. Dry Fluids

In the LERC, the condensation heat comes from two parts: one part is carried by the flow from the generator and the other part is carried by the flow from the evaporator. There is

$$Q_{\text{co}} = \dot{m}_{\text{ev}} q_{\text{co, ev}} + \dot{m}_{\text{ge}} q_{\text{co, ge}} \tag{20}$$

where $q_{\text{co, ev}}$ is the specific condensation heat from the refrigeration part, and $q_{\text{co, ge}}$ is the specific condensation heat from the generation part.

Substituting Equations (8), (10), and (20) into (6), the limiting COP of wetting fluids can be expressed as

$$COP''_{\text{limit}} = \frac{q''_{\text{ev}}}{q_{\text{co, ev}} - q''_{\text{ev}}} \cdot \frac{q''_{\text{ge}} - q_{\text{co, ge}}}{q''_{\text{ge}}} = \left(\frac{q''_{\text{ev}}}{q_{\text{co, ev}} - q''_{\text{ev}}} \right) \left(1 - \frac{q_{\text{co, ge}}}{q''_{\text{ge}}} \right) \tag{21}$$

where

$$q''_{\text{ev}} = A_{6-7-c-a-6} = T_L (s_c - s_a) = T_L \cdot \Delta s_{c-a} \tag{22}$$

$$q_{\text{co, ev}} = A_{7s-1-a-c-7s} = T_M (s_c - s_a) = T_M \cdot \Delta s_{c-a} \tag{23}$$

$$q''_{\text{ge}} = A_{1-3-4-b-a-1} = A_{1s-4-b-a-1s} - A_{1s-3-1-1s} \tag{24}$$

$$q_{\text{co, ge}} = A_{4s-1-a-b-4s} = T_M (s_b - s_a) = T_M \cdot \Delta s_{b-a} \tag{25}$$

$A_{1s-4-b-a-1s}$ and $A_{1s-3-1-1s}$ can be calculated from (17) and (18). Substituting (22)–(25) and into (21), the limiting COP is expressed as:

$$COP''_{\text{limit}} = \frac{T_L}{T_M - T_L} \bullet \left(1 - \frac{T_M}{T_H - \frac{(T_H - T_M)^2}{2\beta \cdot \Delta s_{a-b}}} \right) \tag{26}$$

Comparing (26) and (19), it is found that the expressions of COP_{limit} for wet working fluid, isentropic working fluid, and dry working fluid are the same. Therefore, the limiting COP of ERC be expressed as:

$$COP_{\text{limit}} = \frac{T_L}{T_M - T_L} \bullet \left(1 - \frac{T_M}{T_H - \frac{(T_H - T_M)^2}{2\beta \cdot \Delta s_{a-b}}} \right) \tag{27}$$

COP_{limit} is a function of T_H , T_M , T_L , and β . The greater the slope β and Δs_{a-b} , the greater COP_{limit} .

2.4. Limiting Thermodynamic Perfection

For the ideal ERC, the COP is

$$COP_{\text{ideal}} = \left(\frac{T_H - T_M}{T_H} \right) \left(\frac{T_L}{T_M - T_L} \right) \tag{28}$$

In this research, a parameter named limiting perfection is proposed, which is defined as the ratio between COP_{ideal} and COP_{limit} :

$$\eta_{\text{LTP}} = \frac{COP_{\text{limit}}}{COP_{\text{ideal}}} \times 100\% \tag{29}$$

For actual fluids, η_{LTP} can be an index that reflects its distance to “perfection” in the ERC. It can also evaluate the influence of the working fluid itself on the cycle performance upper limit.

3. Results and Discussion

Based on the above method, the performance of LERC with 15 refrigerants is researched and compared. These fluids are divided into three groups: wet fluids (R290, R134a, and R152a), isentropic fluids (R141b, R142b, R1234yf, and R1234ze), and dry fluids (R600, R245fa, R600a, R601, R236fa, R365mfc, R123, and R227ea). As mentioned above, there is no perfect isentropic fluid whose slope of saturated vapor in the T - s diagram is infinite. Some fluids are approximately regarded as isentropic fluids [26]. In this research, the same method is applied. R141b, R142b, R1234yf, and R1234ze are regarded as isentropic fluids, and the properties of these fluids are listed in Table 1. The effect of operating conditions on COP_{limit} and η_{LTP} are investigated. The referenced operating conditions of T_H , T_L , and T_M are 363.15 K, 303.1 K, and 273.15 K, respectively.

Table 1. The properties of the working fluids researched in this work.

Working Fluid		Environmental and Safety Data [27]			Physical Data [28]		Classification	
Refrigerant number	Chemical formula	ODP	GWP 100yr	Safety group	T_{bo} , K	T_{cr} , K	Slope *	Type
R134a	CH ₂ FCF ₃	0	1370	A1	247.1	374.2	−0.3727	Wet
R152a	CH ₃ CHF ₂	0	133	A2	249.1	386.4	−0.4276	Wet
R290	CH ₃ CH ₂ CH ₃	0	20	A3	231.0	369.9	−0.1225	Wet
R123	CF ₃ CHCl ₂	0.01	77	B1	300.9	456.8	2.4578	Dry
R227ea	CF ₃ CHFCF ₃	0	3580	A1	256.8	374.9	−1.5428	Dry
R236fa	CF ₃ CH ₂ CF ₃	0	9820	A1	271.6	398.1	3.6318	Dry
R245fa	CF ₃ CH ₂ CHF ₂	0	1050	B1	288.2	427.0	1.8363	Dry
R365mfc	CH ₃ CH ₂ CF ₂ CH ₃	0	890	A2	313.3	460.0	0.8124	Dry
R600	CH ₃ CH ₂ CH ₂ CH ₃	0	20	A3	272.6	425.1	0.8897	Dry
R600a	CH(CH ₃) ₂ CH ₃	0	20	A3	261.4	407.8	1.3193	Dry
R601	CH ₃ CH ₂ CH ₂ CH ₂ CH ₃	0	20	A3	309.2	469.7	0.5027	Dry
R141b	CH ₃ CCl ₂ F	0.12	717	\	305.2	477.5	3.2231	Isentropic
R142b	CH ₃ CClF ₂	0.06	2220	A2	264.0	410.3	−7.1431	Isentropic
R1234ze	CHF=CCF ₃	0	6	A2L	254.1	382.5	−1.0939	Isentropic
R1234yf	CH ₂ =CFCF ₃	0	<4.4	A2L	243.6	367.8	−0.2411	Isentropic

* The slope is the saturated vapor slope at 363.15 K.

3.1. Effect of High Temperature

Figure 5 shows the variation in COP_{limit} at different high temperatures for these fluids. As can be seen, when T_H increases from 343.15 to 400.15 K, COP_{limit} increases. This is because when T_H increases, the temperature difference between the middle temperature and high temperature rises. According to Equation (22), the limiting COP increases.

As shown in Figure 5a, for wet fluids, COP_{limit} of R152a is significantly higher than that of R134a and R290. When T_H increases from 343.15 to 383.15 K, its COP_{limit} increases from 0.941 to 1.479. This is because, for R152a, its Δs_{a-b} is much larger than that of R134a. Although smaller than R290, its slope β is greater. For the isentropic fluid group, the COP_{limit} of R141b is the largest, and it is the smallest for R1234yf. This is because the slope and entropy increase Δs_{a-b} of R141b is the largest in this group.

For the dry fluid group, as shown in Figure 5c, the COP_{limit} of R123 is higher than the others, while it is the lowest for R227ea. When T_H increases, COP_{limit} increases from 0.87 to 1.15 for R227ea. For R123, it increases from 0.95 to 2.02, and for R601, COP_{limit} increases from 0.95 to 2.119. The order of COP_{limit} for these eight selected dry fluids is R123>R601>R365mfc>R600>R245fa>R600a>R236fa>R227ea. Among these dry fluids, the slope of R123 is the largest, but Δs_{a-b} of R601 is the largest. The slope of R227ea is only smaller than R123, but its Δs_{a-b} is the smallest. The COP_{limit} differences between these dry

fluids are small at low temperatures, and they increase gradually as T_H increases. It can be seen from Equation (27) that COP_{limit} is a function of high temperature T_H , the slope of the saturated liquid line β , and entropy increase Δs_{a-b} . For wet fluids and isentropic fluids, β and Δs_{a-b} are constant when T_H varies. The COP_{limit} is influenced by T_H . However, for dry fluids, both T_H and Δs_{a-b} change when T_H varies. This results in different COP_{limit} variations for wet fluids, isentropic fluids, and dry fluids.

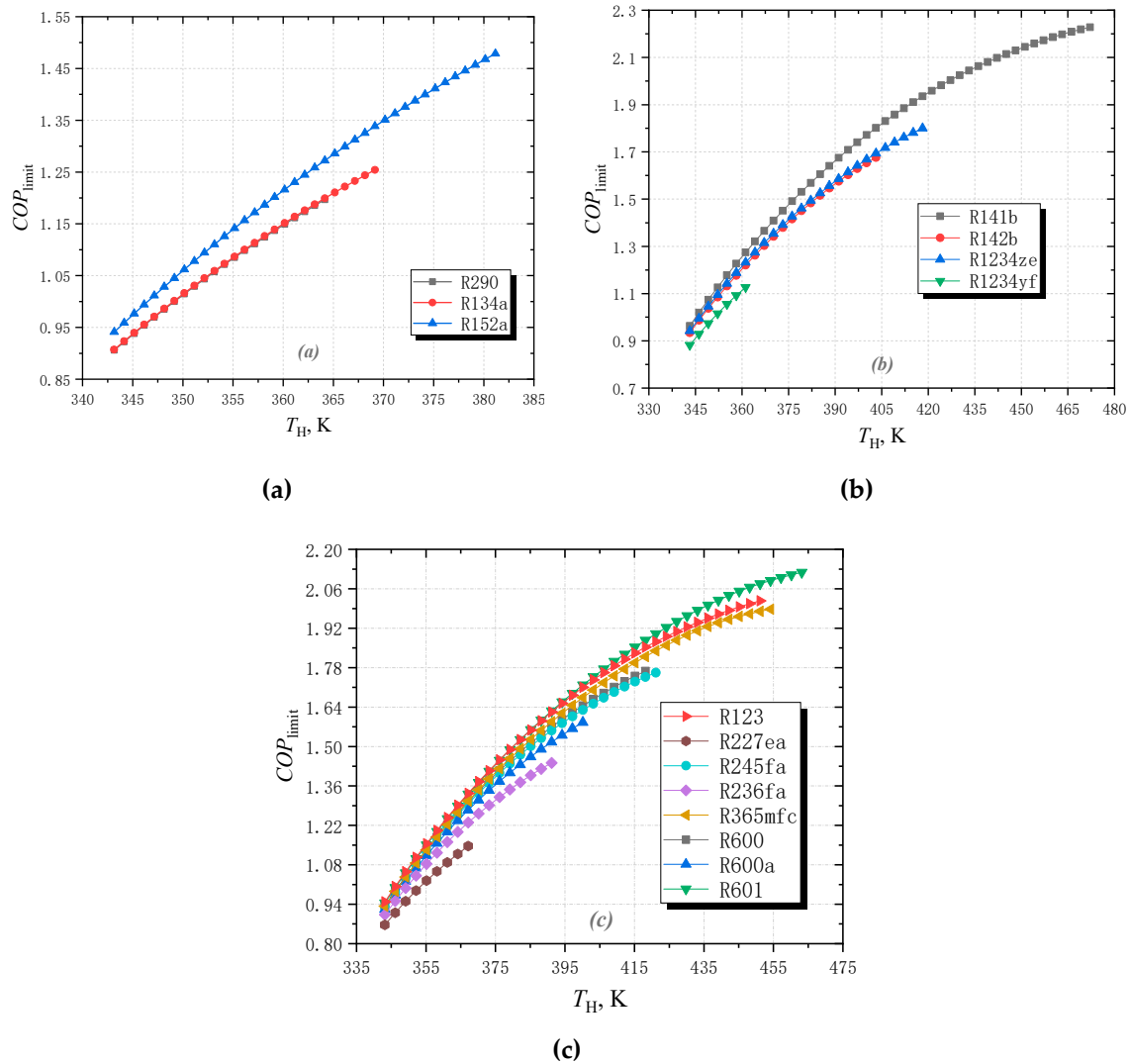


Figure 5. The effect of high temperature on the limiting COP with (a) wet working fluids; (b) isentropic working fluids; (c) dry working fluids.

Figure 6 shows how the limiting thermodynamic perfection η_{LTP} varies with high temperatures for the selected pure fluids. It is found when the T_H increases, η_{LTP} keeps decreasing for all fluids. This is because when T_H increases, as the slope remains the same, the loss caused by the subcooling section increases. This means that the higher the heat source temperature, the larger the gap between the limiting cycle and the ideal cycle. This also indicates that working fluid has a greater negative effect on cycle performance in higher generating temperatures.

The order of η_{LTP} remains the same compared with that of COP_{limit} for all fluids. The difference in η_{LTP} is caused by that of COP_{limit} . Therefore, η_{LTP} has similar variation law of COP_{limit} . For the wet fluid group, the order of η_{LTP} is $R152a > R134a > R290$. For the isentropic fluid group, the order is $R141b > R142b > R1234ze > R1234yf$. For the dry fluid group, the order is $R123 > R601 > R365mfc > R600 > R245fa > R600a > R236fa > R227ea$. R152a, R141b, and

R123 perform best in each group, respectively. The order of η_{LTP} is R141b>R123>R152a, with the value of 86.8%, 84.90%, and 83.67%, separately.

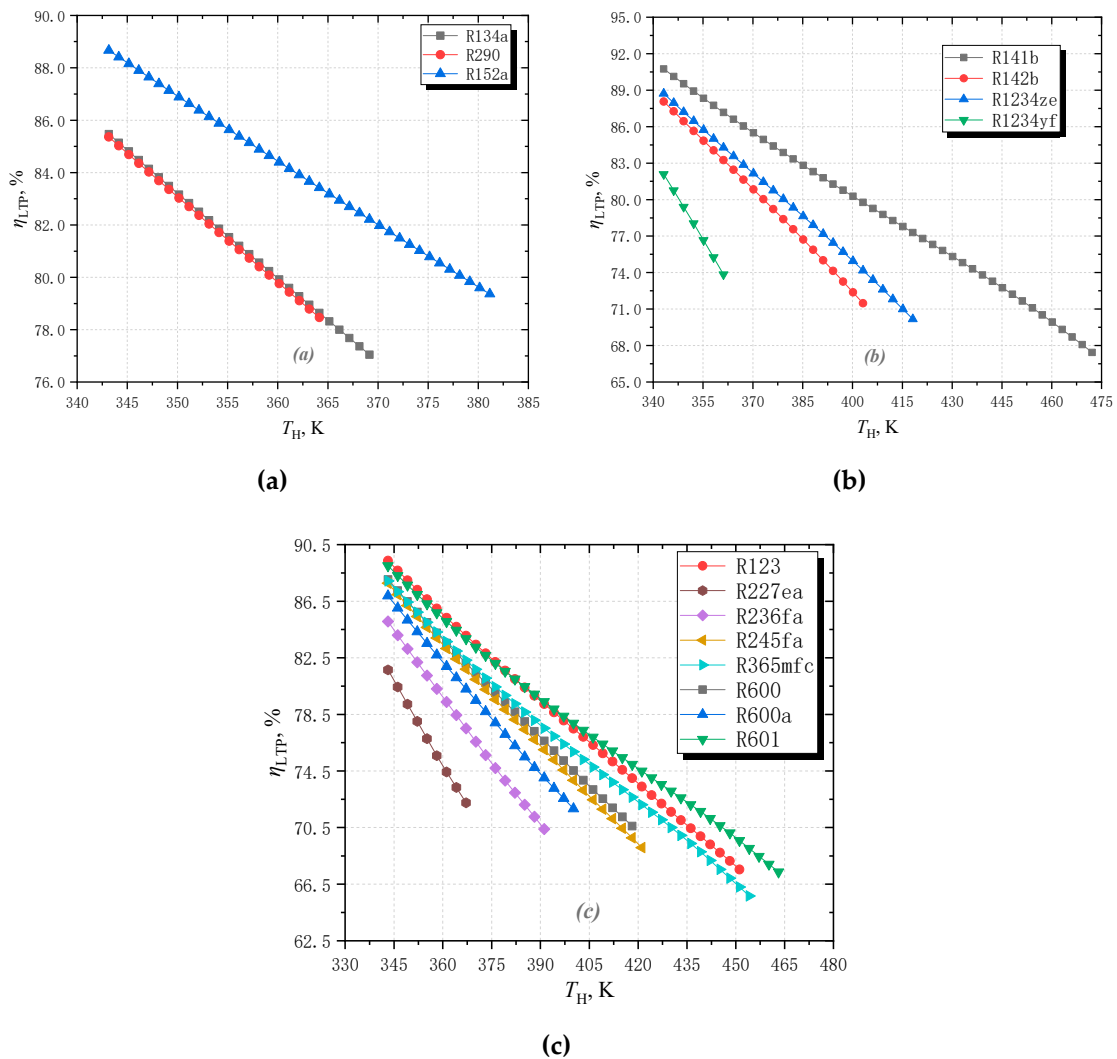


Figure 6. The effect of high temperature on the limiting thermodynamic perfection with (a) wet working fluids; (b) isentropic working fluids; (c) dry working fluids.

3.2. Effect of Middle Temperature

Figures 7 and 8 show the effect of middle temperature T_M on the limiting performance of ERC. It can be seen from Figure 7 that when T_H increases from 298.15 to 308.15 K, COP_{limit} decreases for all fluids. When T_M increases, the temperature difference between middle temperature and low temperature increases. Consequently, the efficiency of the refrigeration part decreases according to Equation (27). At the same time, the temperature difference between the middle temperature and high temperature is reduced, which leads to a reduction in the efficiency of the cycle driving part. Therefore, the efficiency of the entire refrigeration cycle decreases.

As shown in Figure 8, when the middle temperature increases, the thermodynamic perfection for all fluids decrease. When T_M increases, the temperature difference between high temperature and middle temperature decreases. As a result, the irreversibility in the subcooling section of the working fluid decreases accordingly.

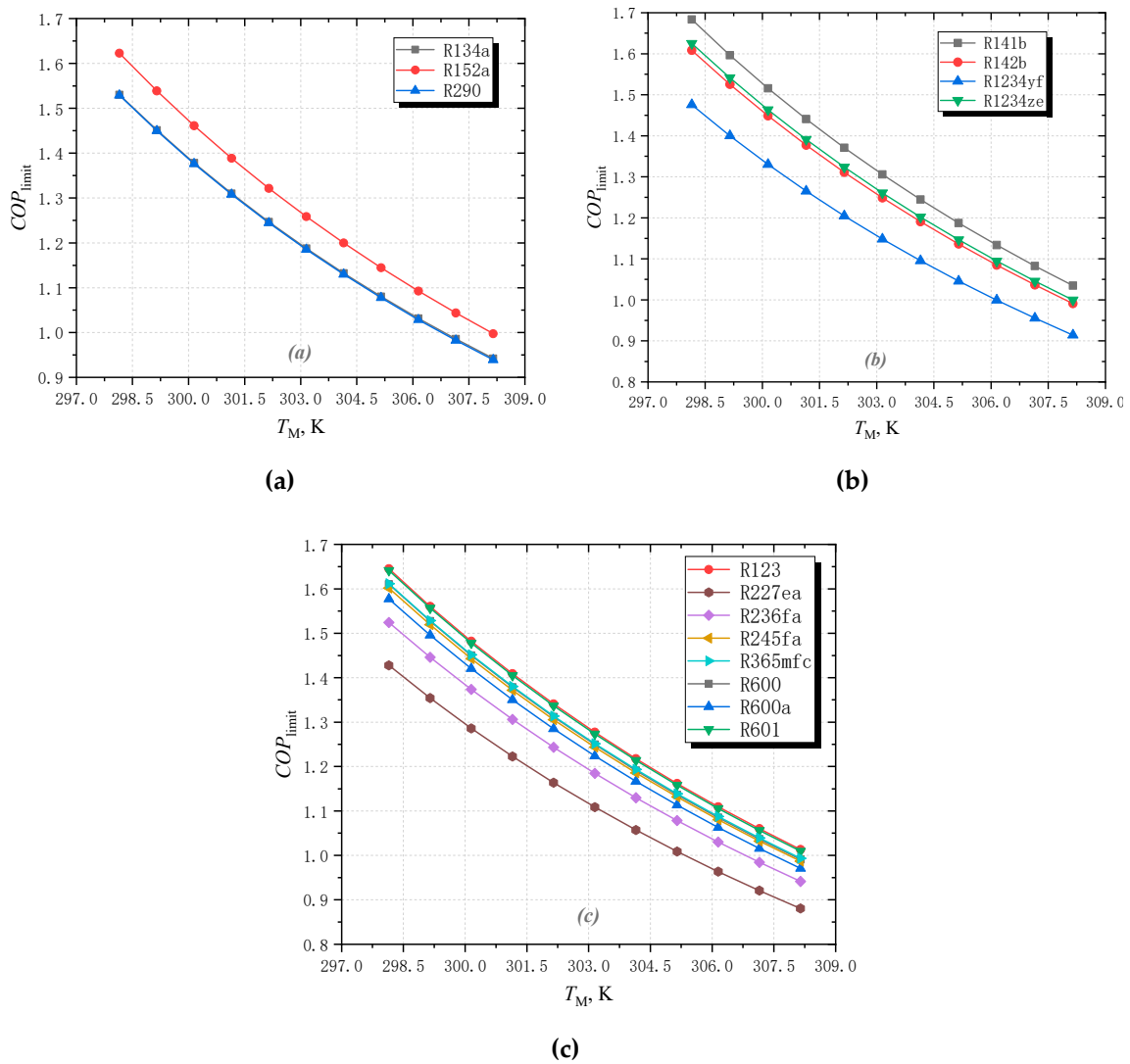


Figure 7. The effect of middle temperature on the limiting COP for different fluids: (a) wet fluids; (b) isentropic fluids; (c) dry fluids.

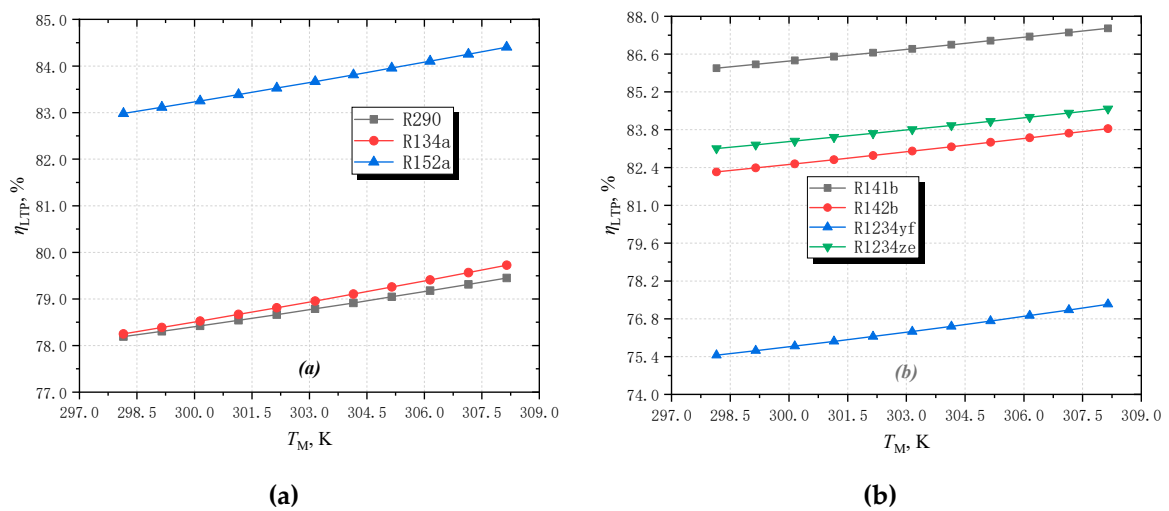
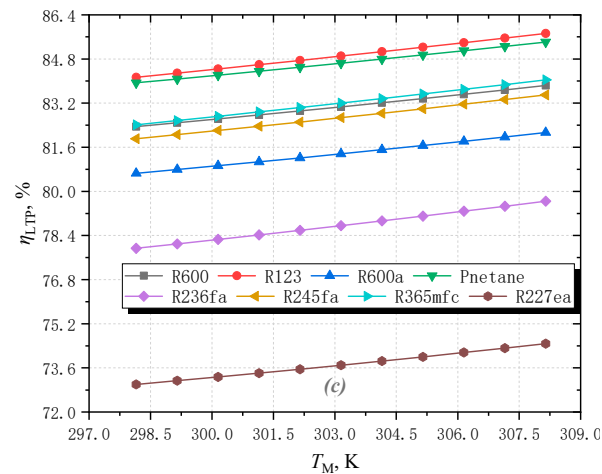


Figure 8. Cont.



(c)

Figure 8. The effect of middle temperature on the limiting perfection with different fluids: (a) wet fluids; (b) isentropic fluids; (c) dry fluids.

4. Conclusions

To evaluate the performance upper limit of ERC with pure fluids quantitatively, a LERC is proposed in this research. Combined with a thermodynamic graphical analysis method, the limiting COP that is expressed by the fluid thermophysical properties and working conditions is derived. And the limiting performance of dry fluids, wet fluids, and isentropic fluids is researched and compared. The key thermophysical parameters of the working fluid that affect COP_{limit} are β and Δs_{a-b} . COP_{limit} is a function of T_H , T_M , T_L , β , and Δs_{a-b} , and COP_{limit} increases with the increase in T_H and T_M for all fluids; however, η_{LTP} decreases as T_H increases. For the wet fluid group, the COP_{limit} and η_{LTP} of R152a are the largest. For the dry fluid group, R123 is better than the others, and η_{LTP} of R141b, R152a, and R123 at the referenced state is 86.8%, 84.90%, and 83.67%, respectively.

Author Contributions: Investigation, J.F.; Methodology, J.F. and X.Y.; data curation, Z.L., X.Y., and J.Y.; writing—original draft preparation, J.F. and X.Y.; writing—review and editing, Z.L. and S.J.; supervision, S.J. and J.Y. All authors have read and agreed to the published version of the manuscript.

Funding: This research received no external funding.

Institutional Review Board Statement: Not applicable.

Data Availability Statement: Not applicable.

Conflicts of Interest: The authors declare no conflict of interest.

Nomenclature

Symbols

A	area
c_p	specific heat capacity at constant pressure ($\text{kJ}\cdot\text{kg}^{-1}\cdot\text{K}^{-1}$)
COP	coefficient of performance
ERC	ejector refrigeration cycle
h_{L-V}	specific heat of vaporization ($\text{kJ}\cdot\text{kg}^{-1}$)
LERC	limiting ejector refrigeration cycle
\dot{m}	mass flow rate ($\text{kg}\cdot\text{s}^{-1}$)
\dot{Q}	heat load (kW)
s	specific entropy ($\text{kJ}\cdot\text{kg}^{-1}\cdot\text{K}^{-1}$)
T	temperature [K]

v	specific volume ($\text{m}^3 \cdot \text{kg}^{-1}$)
α_v	thermal expansion coefficient (1/K)
Greek letters	
β	slope of the oblique line
η	efficiency (%)
μ	entrainment ratio
ζ	relative heat loss ratio
ρ	density (kg/m^3)
Subscripts	
bo	boiling
c	compression
co	condensation
cr	critical
ev	evaporation
ge	generation
H	high temperature in cycle
L	low temperature in cycle
limit	performance limit
LTP	limiting thermodynamic perfection
M	Middle temperature
p	pressure
r	reduced
s	saturated
V	saturated vapor
L	saturated liquid

References

1. Coulomb, D.; Dupont, J.-L.; Pichard, A. *The Role of Refrigeration in the Global Economy—29 Informatory Note on Refrigeration Technologies*; IIF-IIR: Paris, France, 2015; p. 32.
2. Besagni, G.; Mereu, R.; Inzoli, F. Ejector Refrigeration: A Comprehensive Review. *Renew. Sustain. Energy Rev.* **2016**, *53*, 373–407. [[CrossRef](#)]
3. Tashtoush, B.M.; Moh'd A, A.N.; Khasawneh, M.A. A comprehensive review of ejector design, performance, and applications. *Appl. Energy* **2019**, *240*, 138–172. [[CrossRef](#)]
4. Elbel, S.; Hrnjak, P. *Ejector Refrigeration: An Overview of Historical and Present Developments with an Emphasis on Air-Conditioning Applications*; Purdue Universit: West Lafayette, IN, USA, 2008; p. 9.
5. Yapıcı, R.; Yetişen, C.C. Experimental Study on Ejector Refrigeration System Powered by Low Grade Heat. *Energy Convers. Manag.* **2007**, *48*, 1560–1568. [[CrossRef](#)]
6. Dorantès, R.; Lallemand, A. Influence de la nature des fluides, purs ou en mélanges non-azéotropiques, sur les performances d'une machine de climatisation à éjecto-compresseur. *Int. J. Refrig.* **1995**, *18*, 21–30. [[CrossRef](#)]
7. Al-Khalidy, N. An Experimental Study of an Ejector Cycle Refrigeration Machine Operating on R113: Etude Expérimentale d'une Machine Frigorifique à Éjecteur Au R113. *Int. J. Refrig.* **1998**, *21*, 617–625. [[CrossRef](#)]
8. Yan, J.; Chen, G.; Liu, C.; Tang, L.; Chen, Q. Experimental Investigations on a R134a Ejector Applied in a Refrigeration System. *Appl. Therm. Eng.* **2017**, *110*, 1061–1065. [[CrossRef](#)]
9. Huang, B.J.; Chang, J.M.; Wang, C.P.; Petrenko, V.A. A 1-D Analysis of Ejector Performance. *Int. J. Refrig.* **1999**, *22*, 354–364. [[CrossRef](#)]
10. Boumaraf, L.; Lallemand, A. Modeling of an Ejector Refrigerating System Operating in Dimensioning and Off-Dimensioning Conditions with the Working Fluids R142b and R600a. *Appl. Therm. Eng.* **2009**, *29*, 265–274. [[CrossRef](#)]
11. Aghagoli, A.; Sorin, M. CFD Modelling and Exergy Analysis of a Heat Pump Cycle with Tesla Turbine Using CO₂ as a Working Fluid. *Appl. Therm. Eng.* **2020**, *178*, 115587. [[CrossRef](#)]
12. Hamzaoui, M.; Nesreddine, H.; Aidoun, Z.; Balistrrou, M. Experimental Study of a Low Grade Heat Driven Ejector Cooling System Using the Working Fluid R245fa. *Int. J. Refrig.* **2018**, *86*, 388–400. [[CrossRef](#)]
13. Ruangtrakoon, N.; Aphornratana, S. Development and Performance of Steam Ejector Refrigeration System Operated in Real Application in Thailand. *Int. J. Refrig.* **2014**, *48*, 142–152. [[CrossRef](#)]
14. Sankarlal, T.; Mani, A. Experimental Investigations on Ejector Refrigeration System with Ammonia. *Renew. Energy* **2007**, *32*, 1403–1413. [[CrossRef](#)]
15. Kumar, J.; Jain, N. Performance Analysis of Heat Operated Ejector Refrigeration System with Natural Refrigerants R-717 and Propane. *Int. J. Sci. Res.* **2013**, *2*, 139–142.
16. Mwesigye, A.; Dworkin, S.B. Performance Analysis and Optimization of an Ejector Refrigeration System Using Alternative Working Fluids under Critical and Subcritical Operation Modes. *Energy Convers. Manag.* **2018**, *176*, 209–226. [[CrossRef](#)]

17. Pridasawas, W.; Lundqvist, P. A Year-Round Dynamic Simulation of a Solar-Driven Ejector Refrigeration System with Iso-Butane as a Refrigerant. *Int. J. Refrig.* **2007**, *30*, 840–850. [[CrossRef](#)]
18. Zheng, N.; Song, W.; Zhao, L. Theoretical and Experimental Investigations on the Changing Regularity of the Extreme Point of the Temperature Difference between Zeotropic Mixtures and Heat Transfer Fluid. *Energy* **2013**, *55*, 541–552. [[CrossRef](#)]
19. Yang, X.; Xu, J.; Miao, Z.; Zou, J.; Qi, F. The Definition of Non-Dimensional Integration Temperature Difference and Its Effect on Organic Rankine Cycle. *Appl. Energy* **2016**, *167*, 17–33. [[CrossRef](#)]
20. Xu, W.; Zhang, J.; Zhao, L.; Deng, S.; Zhang, Y. Novel Experimental Research on the Compression Process in Organic Rankine Cycle (ORC). *Energy Convers. Manag.* **2017**, *137*, 1–11. [[CrossRef](#)]
21. Chen, J.; Havtun, H.; Palm, B. Screening of Working Fluids for the Ejector Refrigeration System. *Int. J. Refrig.* **2014**, *47*, 1–14. [[CrossRef](#)]
22. Buyadgie, D.; Buyadgie, O.; Artemenko, S.; Chamchine, A.; Drakhnia, O. Conceptual Design of Binary/Multicomponent Fluid Ejector Refrigeration Systems. *Int. J. Low-Carbon Technol.* **2012**, *7*, 120–127. [[CrossRef](#)]
23. Kasperski, J.; Gil, B. Performance Estimation of Ejector Cycles Using Heavier Hydrocarbon Refrigerants. *Appl. Therm. Eng.* **2014**, *71*, 197–203. [[CrossRef](#)]
24. Gil, B.; Kasperski, J. Efficiency Analysis of Alternative Refrigerants for Ejector Cooling Cycles. *Energy Convers. Manag.* **2015**, *94*, 12–18. [[CrossRef](#)]
25. Śmierciew, K.; Pawluczuk, A.; Gagan, J.; Butrymowicz, D. Thermodynamic Analysis of Two-Phase Injector for Various Working Fluids. *Appl. Therm. Eng.* **2019**, *157*, 113713. [[CrossRef](#)]
26. Xu, W.; Deng, S.; Zhao, L.; Su, W.; Zhang, Y.; Li, S.; Ma, M. How to Quantitatively Describe the Role of the Pure Working Fluids in Subcritical Organic Rankine Cycle: A Limitation on Efficiency. *Energy Convers. Manag.* **2018**, *172*, 316–327. [[CrossRef](#)]
27. Calm, J.M.; Hourahan, G.C. Physical, Safety, and Environmental Data for Current and Alternative Refrigerants. In Proceedings of the Proceedings of 23rd International Congress of Refrigeration (ICR2011), Prague, Czech Republic, 21–26 August 2011.
28. Lemmon, E.W.; Huber, M.L.; McLinden, M.O. *NIST Standard Reference Database 23: Reference Fluid Thermodynamic and Transport Properties-REFPROP. 9.0*; National Institute of Standards and Technology: Boulder, CO, USA, 2010.

Disclaimer/Publisher’s Note: The statements, opinions and data contained in all publications are solely those of the individual author(s) and contributor(s) and not of MDPI and/or the editor(s). MDPI and/or the editor(s) disclaim responsibility for any injury to people or property resulting from any ideas, methods, instructions or products referred to in the content.